Polymer 49 (2008) 4877–4881

Contents lists available at ScienceDirect

Polymer

journal homepage: www.elsevier.com/locate/polymer

Lyotropic liquid crystal formation of polystyrene polymacromonomers in dichloromethane

Yo Nakamura*,[1], Miyako Koori, Yu Li, Takashi Norisuye

Department of Macromolecular Science, Osaka University, Machikaneyama-cho, Toyonaka, Osaka 560-0043, Japan

ARTICLE INFO

Article history:
Received 14 May 2008
Accepted 26 August 2008
Available online 11 September 2008

Keywords:
Liquid crystallinity
Polymacromonomer
Phase boundary

ABSTRACT

Liquid crystallinity of dichloromethane (DCM) solutions of five samples of polymacromonomer F65 consisting of 65 styrene residues in each side chain was studied by birefringence observation and phase separation experiments at different temperatures in a molecular weight range from 9.4×10^5 to 4.1×10^6. Dilute-solution characterization was also made by light scattering and viscometry in DCM at 20 °C. The polymer concentration c_I on the phase boundary between the isotropic and biphasic regions was lower than the previously determined c_I for a polymacromonomer with a shorter side-chain length of 33 styrene residues at the same molecular weight, reflecting the higher chain stiffness and larger diameter of the F65 polymer. The molecular weight dependence of c_I for the two polymacromonomers (at 20 °C) was explained almost quantitatively by the scaled-particle theory for worm-like cylinders with the model parameters (the Kuhn length, the linear mass density, and the chain diameter) describing gyration radius and intrinsic viscosity data in DCM but without chain-end effect. It was concluded that this theory is capable of predicting the phase boundary concentration of brush-like polymers with essentially the same degree of accuracy as that known for linear, stiff chains.

1. Introduction

Polymacromonomers, which have a polymeric side chain for every main-chain residue, are known to behave as stiff chains [1–11], whose concentrated solutions are expected to form liquid crystalline phases. Lyotropic liquid crystal (LC) formation of polymacromonomers was reported first by Wintermantel et al. [12] and Tsukahara et al. [13] at about the same time. These groups found that birefringence appears in solutions of polymacromonomers consisting of the poly(methyl methacrylate) main chain and polystyrene side chains at high concentrations, but they did not examine phase boundaries in a quantitative manner.

Previously, we investigated the phase boundary concentration c_I for dichloromethane (DCM) solutions of polymacromonomer SS-33 (or designated F33 in later papers [9,10]) consisting of polystyrene with 33 monomeric units in each side chain [14], where c_I is defined as the polymer mass concentration at which a nematic LC phase starts appearing. The c_I values determined were close to the ones predicted by the scaled-particle theory for worm-like cylinders [15], but the hard-core diameter appearing in the theory had to be assigned about 10% smaller than that expected from intrinsic viscosity ($[\eta]$) data. More importantly, the molecular weight dependence of experimental c_I was rather strong compared to the prediction, suggesting that there exists some problem in applying the theory to brush-like molecules. To examine these matters, we extended the work to a polystyrene polymacromonomer (F65) with a longer side chain of 65 monomeric units. This paper reports dilute-solution characterization of the F65 polymacromonomer in DCM, its liquid crystallinity at high concentrations, and a comparison of c_I with the prediction from the scaled-particle theory. The previous c_I data for the SS-33 polymer [14] are also analyzed.

2. Experimental section

2.1. Samples

Polymacromonomer samples F65-2, F65-3, F65-4, and F65-6 were chosen from those used in our previous work [9], and added to them was a new sample F65-C5, a previously prepared middle fraction. The weight-average molecular weights M_w and the number to weight-average molecular weight ratios M_w/M_n determined previously [9] from light scattering and size-exclusion chromatography are presented in Table 1.

* Corresponding author. Tel.: +81 75 383 2625; fax: +81 75 383 2628.
E-mail address: yonaka@molsci.polym.kyoto-u.ac.jp (Y. Nakamura).
[1] Present address: Department of Polymer Chemistry, Kyoto University, Katsura, Kyoto 615-8510, Japan.

0032-3861/$ – see front matter © 2008 Elsevier Ltd. All rights reserved.
doi:10.1016/j.polymer.2008.08.049

Table 1
Results from light scattering, viscometry, and phase separation experiments for samples of polystyrene polymacromonomer F65 in DCM at 20 °C

Sample	$M_w/10^5$	M_w/M_n	$\langle S^2\rangle/10^2$ nm^2	$[\eta]$/cm^3 g^{-1}	c_I/g cm^{-3}	c_A/g cm^{-3}
F65-2	40.6[a]	1.10[a]	—	40.7	0.163	0.169
F65-3	36.6[a]	1.09[a]	—	30.0	0.156	—
F65-4	21.3	1.09[a]	4.1_1	21.8	0.168	0.173
F65-C5	13.2	—	2.0	15.7	0.202	—
F65-6	9.43[a]	1.27[a]	—	14.2	0.227	0.233

[a] Ref. [9].

2.2. Light scattering

Light scattering measurements were made on a Fica-50 light scattering photometer with vertically polarized incident light of 436-nm wavelength for samples F65-4 and F65-C5 in DCM at 20 °C to determine M_w and the mean-square radius of gyration $\langle S^2\rangle$ (see Refs. [5,9] for the experimental procedures). The refractive index increment for DCM solutions at 436 nm was taken to be 0.181 cm^3 g^{-1} [14].

2.3. Viscometry

Solution viscosity for each sample in DCM at 20 °C was measured by use of a Ubbelohde type capillary viscometer. Huggins [16], Fuoss and Mead [17], and Billmeyer [18] plots were combined to determine $[\eta]$ from their common intercept.

2.4. Determination of phase boundary concentrations

A DCM solution of a given F65 polymacromonomer sample in a test tube (8 mm inner diameter) with a stopcock and a stirring bar at the bottom was placed in a temperature-controlled water bath. A polarizer and an analyzer were set on the front and rear sides of the bath under the cross-polar condition. A tungsten lamp was used to detect birefringence of the solution, i.e., nematic LC formation. The polymer mass concentration c was successively raised by evaporation of the solvent, and was calculated from the gravimetrically determined polymer weight fraction w multiplied by the solution density ρ, which was evaluated according to the relation

$$\rho = \rho_0/[1 - w + \bar{v}\rho_0 w] \quad (1)$$

Here, ρ_0 and $\bar{v}$ are the solvent density and the partial specific volume of the polymer, respectively; for the latter, the literature value 0.911 cm^3 g^{-1} (at 20 °C) [14] was used. As was the case for polymacromonomer SS-33 [14], c_I for F65 depended weakly on temperature T. Thus, we were able to determine the temperature at which the LC phase starts appearing for a given solution upon cooling. This temperature and that at which the LC phase disappears on elevating T agreed within ±0.5 °C. For sample F65-4 the experiment was also performed for toluene solutions.

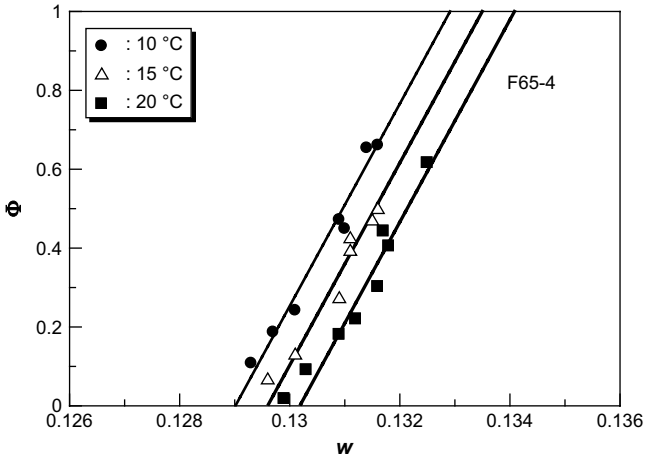

Fig. 1. Volume ratio of the liquid crystalline phase in biphasic solutions plotted against polymer weight fraction for polystyrene polymacromonomer sample F65-4 in DCM.

2.5. Phase equilibrium experiment

A test solution with c slightly above c_I in a test tube was centrifuged for 30 min at 4000 rpm. The tube was then moved into a water bath controlled at the same temperature as in the centrifugation chamber. The height of the solution meniscus and that of the phase boundary from an indicated base line on the tube surface were measured by use of a traveling microscope. The relation between the solution height and its volume was calibrated with pure DCM. The volume ratio Φ of the LC phase to the total solution was measured as a function of polymer concentration. Fig. 1 shows plots of Φ against w for F65-4 in DCM at different temperatures. The data points for each T can be fitted by a straight line whose intercepts at $\Phi = 0$ and 1 give, respectively, c_I and the mass concentration c_A at which the isotropic phase disappears.

3. Results and discussion

3.1. Molecular characteristics

Numerical results of M_w, $\langle S^2\rangle$, and $[\eta]$ for polymacromonomer F65 samples in DCM are summarized in Table 1. Fig. 2 shows that these $\langle S^2\rangle$ data (filled circles) fall on a curve closely fitting our previous data in toluene [9] (unfilled circles). This curve actually represents the theoretical values calculated from the Benoit–Doty expression [19] for $\langle S^2\rangle_{KP}$ ($\langle S^2\rangle$ of the Kratky–Porod worm-like chain [20]) with the chain thickness [21] and the end effect [7] incorporated, i.e., from

$$\langle S^2\rangle = \langle S^2\rangle_{KP} + d^2/8 \quad (2)$$

and

$$L = M/M_L + \delta \quad (3)$$

for the stiffness parameter (twice the persistence length) $\lambda^{-1} = 75$ nm [9], the linear mass density $M_L = 26000$ nm^{-1}, the chain diameter $d = 12$ nm, and the chain-end parameter $\delta = 3$ nm.

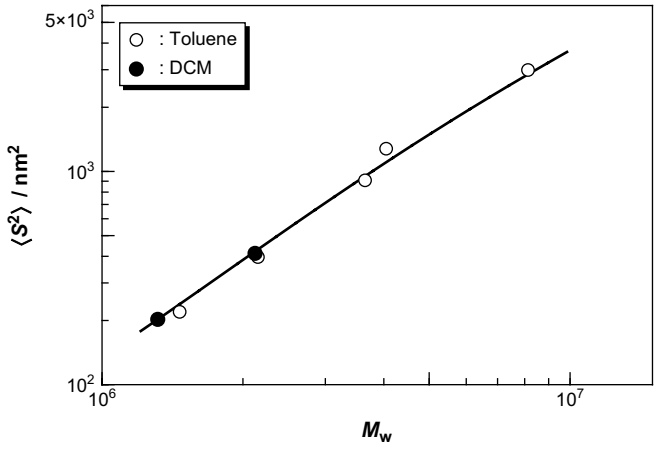

Fig. 2. Molecular weight dependence of mean-square radius of gyration for polystyrene polymacromonomer F65 in DCM at 20 °C (filled circles) and in toluene at 15 °C (unfilled circles) [9]. Curve, Eq. (2) for the cylindrical worm-like chain with $\lambda^{-1} = 75$ nm, $M_L = 26{,}000$ nm^{-1}, $d = 12$ nm, and $\delta = 3$ nm.

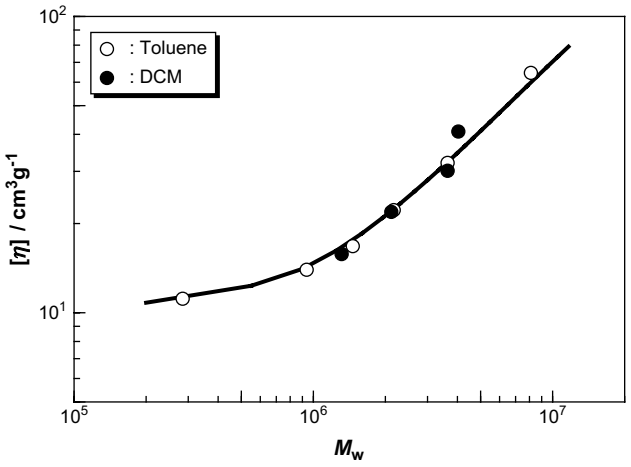

Fig. 3. Molecular weight dependence of intrinsic viscosity for polystyrene polymacromonomer F65 in DCM at 20 °C (filled circles) and in toluene at 15 °C (unfilled circles) [9]. Curve, Yoshizaki, Nitta, and Yamakawa's theory [22] for the touched-bead worm-like chain with $\lambda^{-1}=75$ nm, $M_L=25{,}000$ nm^{-1}, $d=14$ nm, and $\delta=6$ nm.

Here, M denotes the molecular weight and δ represents the apparent contribution of side chains near the main-chain ends to the contour length L (see Fig. 3 of Ref. [7]). The fit of the curve to both filled and unfilled circles suggests that the backbone stiffness and global conformation are essentially the same in the two solvents, as was the case for SS-33 in toluene and DCM [14].

In Fig. 3, $[\eta]$ data for F65 in DCM and toluene (filled and unfilled circles, respectively) form a composite curve, which represents the Yoshizaki–Nitta–Yamakawa theory [22] for the touched-bead worm-like chain with the previously determined parameter set in toluene [9], i.e., $\lambda^{-1}=75$ nm, $M_L=25{,}000$ nm^{-1}, $d=14$ nm, and $\delta=6$ nm. The close fit of this curve to the data points along with the good agreement of the model parameters with those chosen for $\langle S^2\rangle$ confirms the above suggestion (from $\langle S^2\rangle$) that there is no substantial difference in the chain conformation between DCM and toluene.

3.2. Phase boundaries

The unfilled circles in Fig. 4 show the relations between T and c_I determined by birefringence observation for F65 samples in DCM. They follow a straight line as indicated for each sample. The filled squares in the figure show that the phase boundary concentrations for toluene solutions of sample F65-4 are slightly higher than those in DCM. This may be a reflection that DCM is a better solvent than toluene, as revealed for SS-33 by second virial coefficients systematically larger in DCM [14] than in toluene [6].

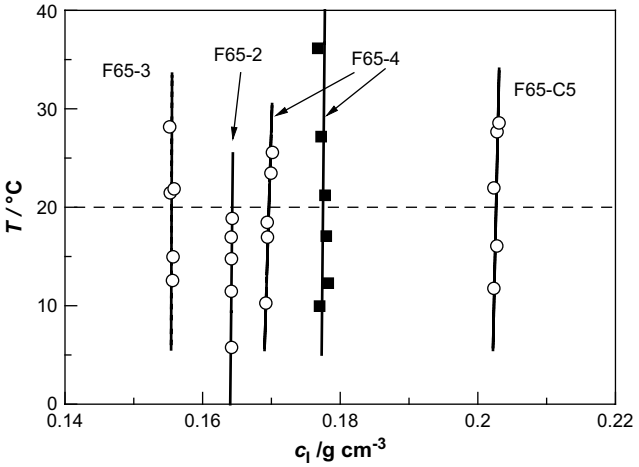

Fig. 4. Relations between T and c_I for indicated F65 polymacromonomer samples in DCM (circles) and toluene (squares), determined by observation of birefringence.

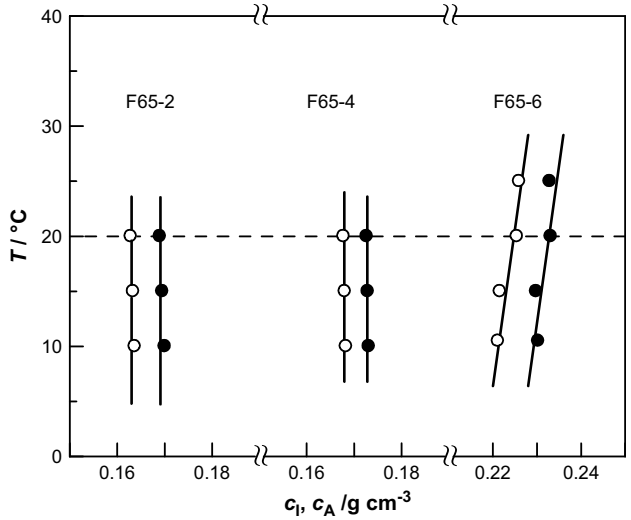

Fig. 5. Relations between T and c_I (unfilled circles) and between T and c_A (filled circles) for indicated F65 polymacromonomer samples in DCM, determined from phase separation experiments.

Fig. 5 illustrates the relations between T and c_I (unfilled circles) and between T and c_A (filled circles) determined from phase separation experiments for F65-2, F65-4, and F65-6, where the left area of the c_I line and the right area of the c_A line correspond to the isotropic and entirely anisotropic regions, respectively, and the area between them represents the two-phase region. This phase gap between the c_I and c_A lines is confined in a very narrow concentration region for any sample. We note that the c_I lines for samples F65-2 and F65-4 determined from the phase separation experiments and birefringence observation agree well with each other.

The values of c_I and c_A for F65 at 20 °C are presented in the sixth and seventh columns of Table 1, respectively, and the molecular weight dependence of c_I is shown by circles in Fig. 6. As is the case

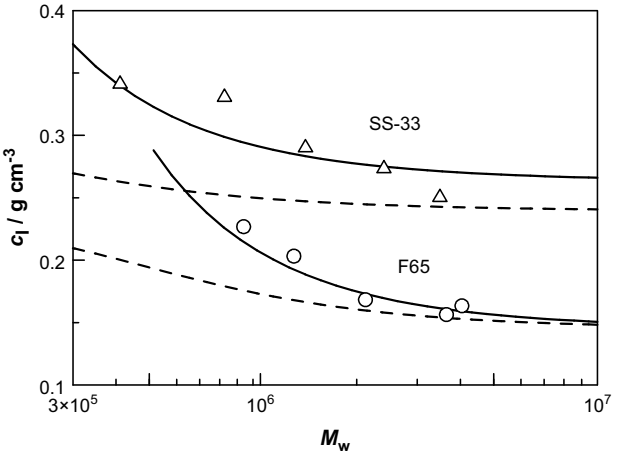

Fig. 6. Molecular weight dependence of c_I for polymacromonomers F65 (circles) and SS-33 (triangles) [14] in DCM at 20 °C, compared with the predictions from the scaled-particle theory [15] for worm-like cylinders with and without chain-end effect (dashed and solid lines, respectively). See the text for the model parameters used.

Table 2
Phase boundary concentrations for samples of polystyrene polymacromonomer SS-33 in DCM at 20 °C [14]

Sample	$M_w/10^5$	c_I/g cm^{-3}
SS-33-1015	34.9	0.250
SS-33-698	24.0	0.273
SS-33-413	14.2	0.290
SS-33-240	8.26	0.331
SS-33-119	4.11	0.341

for linear stiff polymers [15], c_I decreases with increasing M_w and the decrease becomes gradual at high M_w. For comparison, our previous c_I data for the SS-33 polymacromonomer in DCM at 20 °C are shown by triangles in Fig. 6. At a given M_w, c_I for F65 is considerably lower than that for SS-33, reflecting the higher backbone stiffness and the larger chain diameter of the F65 polymer. It should be noted that the difference in c_I between the two polymers is more pronounced when comparison is made at the same contour length. The numerical data of c_I for SS-33, not presented in the previous paper [14], are listed in Table 2 for reference.

We also investigated anisotropy for DCM solutions of an F65 sample with a lower M_w of 2.4×10^5 in the hope of extending the molecular weight range of experimental c_I, but we found that the solution lost fluidity at about $w = 0.4$ ($c \sim 0.5$ g cm^{-3}) without forming LC phase. Similar gel-like behavior was also observed for isotropic solutions of SS-33 in carbon tetrachloride and 1,2-dichloroethane and for LC phases of SS-33 in DCM and chloroform [14] in contrast to the high fluidity of LC phases of typical stiff-polymer solutions. These findings suggest the presence of some special interaction among polymacromonomer molecules in concentrated solutions.

3.3. Comparison with the scaled-particle theory

Sato and Teramoto [15] showed that phase boundary concentrations for various semiflexible and rigid polymers are explained almost quantitatively by the scaled-particle theory for worm-like cylinders with intermolecular hard-core interactions. In Fig. 6, the dashed line for F65 representing the theoretical c_I for the parameter set from the $[\eta]$ data in Fig. 3 ($d = 14$ nm, $\delta = 6$ nm, $\lambda^{-1} = 75$ nm, and $M_L = 25{,}000$ nm^{-1}) appears considerably below the circles. If we take $d = 13$ nm, the theoretical line comes close to the data points (not shown), but the molecular weight dependence is still appreciably weaker than the experimental relation. A similar tendency was previously observed for c_I of SS-33 in DCM, as is shown by the upper dashed line in Fig. 6 for $d = 8.5$ nm, $\delta = 4.3$ nm, $\lambda^{-1} = 36$ nm, and $M_L = 13{,}800$ nm^{-1} (determined from $[\eta]$ [7,14]); a smaller d of 7.5 nm led the theoretical curve to come closer to the data points, but the molecular weight dependence remained weak [14].

The hard-core diameter appearing in the scaled-particle theory cannot unequivocally be defined for the F65 or SS-33 polymacromonomer, because every side chain is long and not quite rigid [11]. The same is true for the apparent contribution to L defined in Eq. (3). It is thus legitimate to regard both d and δ as adjustable parameters in the present analysis even though DCM is a better solvent than toluene, a typical good solvent for polystyrene.

The solid line for F65 in Fig. 6, calculated from the scaled-particle theory for $\delta = 0$ with the other parameters fixed to those for the lower dashed curve, satisfactorily fits the circles. This is also the case for SS-33, for which the upper solid line fitting the triangles has been computed with $\delta = 0$, $d = 8.0$ nm, and the same λ^{-1} and M_L values as those for the upper dashed line. Except for δ, the model parameters used for the calculations are exactly or essentially the same as those explaining the molecular weight dependence of $[\eta]$ or $\langle S^2 \rangle$. We may therefore conclude that the scaled-particle theory is capable of quantitatively describing the chain length dependence of c_I for DCM solutions of polystyrene polymacromonomers F65 and SS-33 without chain-end effect as in the case of linear, stiff or rigid polymers. We note that the c_A values for the three F65 samples (see Table 1) are also in substantial agreement with the theoretically predicted ones (not shown in Fig. 6 for clarity).

In a series of studies, we have demonstrated the significance of δ in discussing hydrodynamic [7–11] and dimensional [23,24] properties of polymacromonomers in dilute solution. In particular, this chain-end parameter was essential for explaining the observed minimum in $\log[\eta]$ vs. $\log M_w$ relations at relatively low molecular weights (see Ref. [11]). On the other hand, the above analysis reveals that δ hardly contributes to the total interaction among polymacromonomer molecules. This is probably because the intermolecular interactions associated with side chains near the main-chain ends are counted in those associated with the cylinder portion. In other words, the spatial distribution of such side chains has almost nothing to do with the total intermolecular interaction, whereas it significantly affects the average size of a relatively short polymacromonomer chain.

4. Conclusions

We have studied LC formation of concentrated DCM solutions of polymacromonomer F65 with 65 styrene units in each side chain. The phase boundary concentration c_I at which the LC phase starts to appear is lower than that for polymacromonomer SS-33 with 33 styrene units in each side chain when compared at the same molecular weight. For both polymers the c_I values are systematically larger than those predicted by the scaled-particle theory of Sato and Teramoto [15] for worm-like cylinders and their molecular weight dependence is stronger than the prediction if the model parameters explaining the molecular weight dependence of $[\eta]$ are used. Quantitative agreement in c_I between theory and experiment is obtained when the chain-end parameter is taken to be zero with the other (worm-like chain) parameters kept essentially unchanged. This finding implies that, while the hydrodynamic and dimensional properties of a single polymacromonomer chain of relatively low molecular weight are significantly affected by the spatial distribution of side chains near the main-chain ends, the total intermolecular interaction potential among them is insensitive to whether those side chains contribute to d or L. The present study demonstrates for the first time that the scaled-particle theory allows the phase boundary concentrations of brush-like polymers to be described by a set of worm-like chain parameters (λ^{-1}, M_L, and d) with essentially the same degree of accuracy as that known for linear, stiff chains [15].

Acknowledgement

We thank Professor Takahiro Sato of Osaka University for valuable discussions.

References

[1] Wintermantel M, Schmidt M, Tsukahara Y, Kajiwara K, Kohjiya S. Macromol Rapid Commun 1994;15:279–84.
[2] Nemoto N, Nagai M, Koike A, Okada S. Macromolecules 1995;28:3854–9.
[3] Wintermantel M, Gerle M, Fischer K, Schmidt M, Wataoka I, Urakawa H, et al. Macromolecules 1996;29:978–83.
[4] Kawaguchi S, Akaike K, Zhang Z-M, Matsumoto H, Ito K. Polym J 1998;30:1004–7.
[5] Terao K, Takeo Y, Tazaki M, Nakamura Y, Norisuye T. Polym J 1999;31:193–8.
[6] Terao K, Nakamura Y, Norisuye T. Macromolecules 1999;32:711–6.
[7] Terao K, Hokajo T, Nakamura Y, Norisuye T. Macromolecules 1999;32:3690–4.
[8] Terao K, Hayashi S, Nakamura Y, Norisuye T. Polym Bull 2000;44:309–16.
[9] Hokajo T, Terao K, Nakamura Y, Norisuye T. Polym J 2001;33:481–5.
[10] Hokajo T, Hanaoka Y, Nakamura Y, Norisuye T. Polym J 2005;37:529–34.
[11] Sugiyama M, Nakamura Y, Norisuye T. Polym J 2008;40:109–15.

[12] Wintermantel M, Fischer K, Gerle M, Ries R, Schmidt M, Kajiwara K, et al. Angew Chem Int Ed Engl 1995;34:1472–4.
[13] Tsukahara Y, Ohta Y, Senoo K. Polymer 1995;36:3413–6.
[14] Maeno K, Nakamura Y, Terao K, Sato T, Norisuye T. Kobunshi Ronbunshu 1999;56:254–9.
[15] Sato T, Teramoto A. Adv Polym Sci 1996;126:87–161.
[16] Huggins ML. J Am Chem Soc 1942;64:2716–8.
[17] Mead DF, Fuoss R. J Am Chem Soc 1942;64:277–82.
[18] Billmeyer Jr FW. J Polym Sci 1949;4:83–6.
[19] Benoit H, Doty P. J Phys Chem 1953;57:958.
[20] Kratky O, Porod G. Recl Trav Chim 1949;68:1106–22.
[21] Konishi T, Yoshizaki T, Saito T, Einaga Y, Yamakawa H. Macromolecules 1990;23:290–7.
[22] Yoshizaki T, Nitta I, Yamakawa H. Macromolecules 1988;21:165–71.
[23] Amitani K, Terao K, Nakamura Y, Norisuye T. Polym J 2005;37:324–31.
[24] Nakamura Y, Sugiyama M, Amitani K, Norisuye T. Polym J 2007;39:1098–104.